Reflectivity of bismuth germanate

F. Antonangeli, N. Zema, and M. Piacentini*
Istituto di Struttura della Materia, Consiglio Nazionale delle Ricerche, via Enrico Fermi 38, I-00044 Frascati (Roma), Italy

U. M. Grassano
Dipartimento di Fisica, Università degli Studi di Roma II, Tor Vergata, via Orazio Raimondo, I-00183 Roma, Italy
(Received 31 July 1987)

We have measured the reflectivity of $Bi_4Ge_3O_{12}$ single crystals at 300 and 80 K from 4 to 40 eV. Beyond the first sharp peak at 4.57 eV, assigned to an excitonic transition, several other structures have been found between 5 and 10 eV, followed by a broad reflectivity band with maximum at about 15 eV. These structures have been assigned to transitions from energy bands derived mainly from the O $2p$ states and the Ge—O bonding states. Further sharp features with the Fano resonance line shape detected around 30 eV have been assigned to core excitons associated with the Bi $5d$ levels. From our assignments we propose a simple model for the density of states of the valence bands and lowest conduction bands of $Bi_4Ge_3O_{12}$.

I. INTRODUCTION

A strong interest exists for bismuth germanate $Bi_4Ge_3O_{12}$ (usually abbreviated as BGO), a transparent material with important applications as x- or γ-ray scintillator or as a laser host material. For these reasons, the emission properties of BGO crystals have been investigated in detail under a variety of excitation methods.[1-3] However, the interpretation of the observed spectra is still rather controversial,[2,3] due to the lack of an adequate model for its electronic energy bands as well as for its excited states.

Since the optical properties of a material are directly linked to its electronic properties, we have measured the reflectivity spectra of $Bi_4Ge_3O_{12}$ single crystals at 80 K and room temperature from the absorption threshold ($\sim$4.1 eV) to about 40 eV. From the reflectivity spectra we have derived the spectra of the other optical constants by means of the Kramers-Kronig transformations. The experimental setup and the results are described in Sec. II. In Sec. III we compare the spectra with previously measured optical constants of BGO in the lowest-energy region of the spectrum,[2-7] and we discuss them, proposing a simple model of the electronic energy levels.

II. EXPERIMENTAL SETUP AND RESULTS

The reflectivity measurements have been performed on the vacuum ultraviolet beam line at the Italian synchrotron radiation facility Programma per l'Utilizzazione della Luce di Sincrotrone (PULS).[8] The radiation from the ADONE storage ring of the Frascati National Laboratories of the Istituto Nazionale di Fisica Nucleare is focused onto the entrance slit of a 1-m normal-incidence monochromator. The entire spectral range 4–40 eV has been scanned using two different gratings and detectors. From 4 eV to 10 eV we used a 600-line/mm aluminum-coated holographic grating and a solar-blind photomultiplier with a LiF window. Above 10 eV we used a 1440-line/mm platinum-coated grating and an electron multiplier with a tungsten photocathode.

The samples were attached to the bottom of a liquid-nitrogen cryostat inside the vacuum chamber. Two samples have been used for this experiment, both prepared by cutting and polishing the same piece of BGO obtained from Harshaw Chemical Co. The reflectivity spectra changed somewhat from the first to the second sample. In Fig. 1 we present the reflectivity spectra measured at 80 K and at room temperature (RT) for the second sample from 4 to 40 eV. The low-energy portions of these spectra are displayed on an expanded scale in Fig. 2. The reflectivity spectrum of the first sample has the same structures as those of the second one, but broader and less resolved. The energies of the most relevant structures, labeled A–H and a_1,a_2,a_3 in Fig. 1, are listed in Table I.

From the reflectivity spectra we derived the other optical constants of BGO by means of the Kramers-Kronig relations. The low-energy extrapolation has been obtained by smoothly connecting our reflectivity data with the reflectivity that we calculated from the values of the index of refraction reported by Bortfeld and Meier.[4] Above 40 eV, the high-energy tail has been parametrized as $R(E)=BE^{-a}$, using the exponent a as a free parameter. By changing the value of a between 1 and 3, the Kramers-Kronig results changed little over the entire spectral range. We think that this is due to the large oscillator strength still existing above 40 eV. The results presented below have been calculated using $a=2$, a value chosen in part for the best shape obtained around the absorption threshold and in part for comparison with model calculations. In Fig. 3 we show the curves for ϵ_1 and ϵ_2, the real and imaginary parts of the dielectric function, respectively, and in Fig. 4 the spectrum of $N_{\rm eff}$, derived from the low-temperature reflectivity. $N_{\rm eff}(\hbar\omega)$ is the effective number of electrons contributing to the total os-

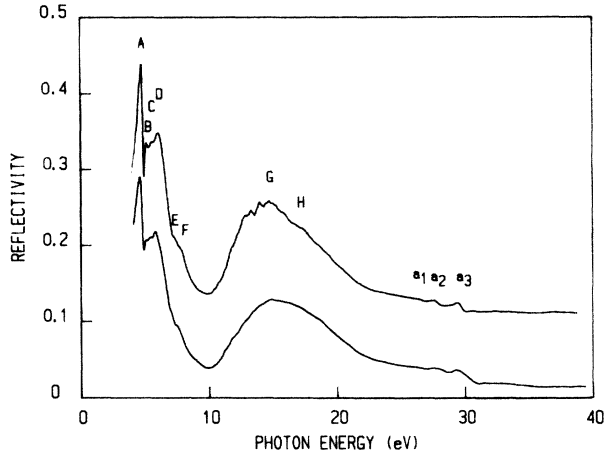

FIG. 1. Reflectivity spectra of a single crystal of $Bi_4Ge_3O_{12}$ measured at room temperature (lower curve) and at 80 K (upper curve). The upper curve has been shifted upwards by 0.1 for a better display.

cillator strength up to energy $\hbar\omega$. The energies of the structures shown in the ϵ_2 spectrum are very close to those of the reflectivity structures and are not reported in Table I.

To our best knowledge, the reflectivity of BGO has been measured previously only at RT up to about 200 nm.[2,5,6] Weber and Monchamp[5] and Moncorgé *et al.*[6] observed a maximum at about 268 nm, followed by a minimum at about 250 nm, in agreement with our peak *A* and the next dip. The reflectivity spectrum measured by Rogemond *et al.*[2] to higher energies (5×10^4 cm^{-1}), shows a second, high-energy peak at 6 eV, which might correspond to our broad reflectivity band between 5 and 6 eV enclosing the structures *B*, *C*, and *D*. The

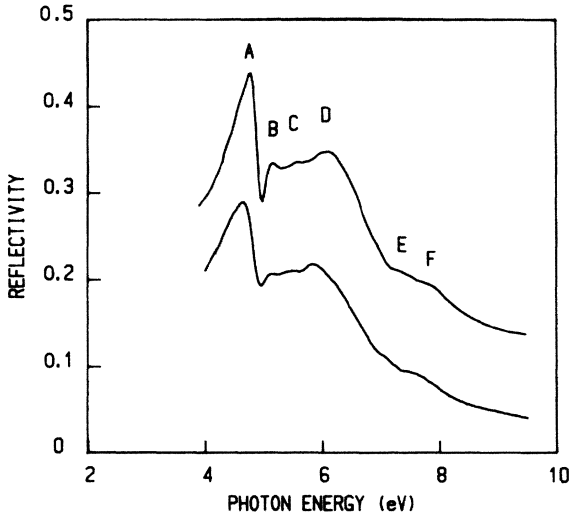

FIG. 2. The low-energy portion of the reflectivity spectra of a single crystal of $Bi_4Ge_3O_{12}$ measured at room temperature (lower curve) and at 80 K (upper curve). The upper curve has been shifted upwards by 0.1 for a better display.

TABLE I. Energies in eV of the structures observed in the reflectivity spectra of $Bi_4Ge_3O_{12}$ at room temperature (RT) and at 80 K.

Structure	RT	80 K
A	4.64	4.78
B	5.10	5.16
C	5.5	5.58
D	5.85	6.10
E	7.03	7.36
F	7.53	7.86
G	15.0	14.7
H		16.9
a_1	26.34	26.20
a_2	27.85	27.58
a_3	29.60	29.43

reflectivity spectra reported by these three groups[2,5,6] present a further low-energy structure, below the absorption threshold, missing in our spectrum. This structure might be due to the enhancement of the reflected intensity due to the reflectivity of the back surface of the sample.

III. DISCUSSION

The interpretation of the optical properties of BGO is quite difficult due to the lack of energy bands or schematic energy-level sequences for this compound. For this reason we shall suggest an interpretation of the gross features of the spectra without attempting to assign the fine structures. Looking at Figs. 1 and 2, we can distinguish four relevant groups of structures: the strong peak *A* at 4.78 eV (80 K), the group of structures *B*–*F* between 5 and 10 eV, the broad band *G* with the maximum at about 14.7 eV followed by the shoulder *H*, and the weak features a_1,a_2,a_3, followed by a steplike decrease, between 25 and 32 eV. The same groups of structures

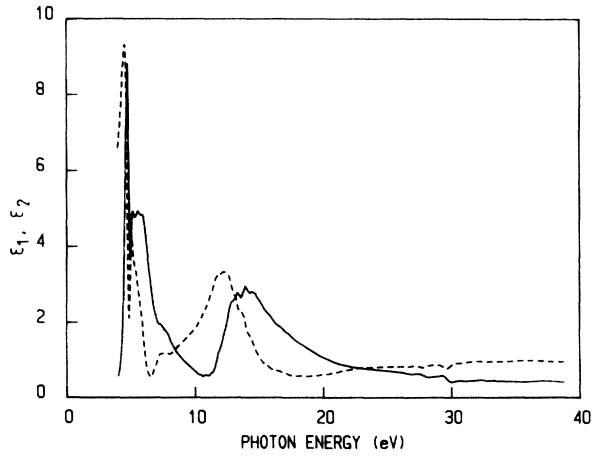

FIG. 3. Spectra of the real (ϵ_1—dashed line) and imaginary (ϵ_2—solid line) parts of the dielectric function of $Bi_4Ge_3O_{12}$ obtained from the Kramers-Kronig transformations of the 80-K reflectivity spectrum.

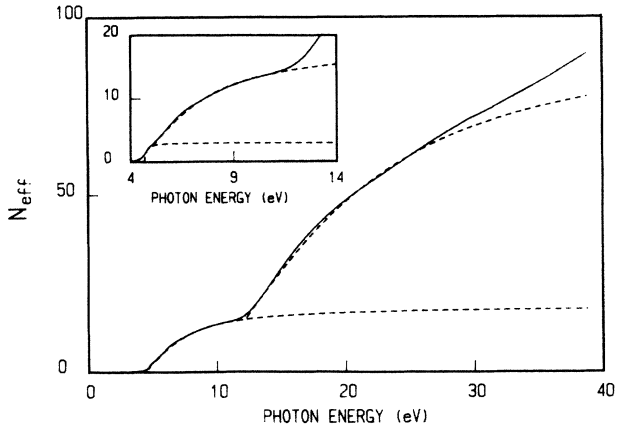

FIG. 4. Spectrum of the effective number N_{eff} of electrons contributing to to the total oscillator strength up to energy $\hbar\omega$, obtained from the Kramers-Kronig transformations of the reflectivity spectrum measured at 80 K. An enlargement of the low-energy portion is presented in the inset. The dashed lines show the partial contributions to N_{eff} obtained from a model calculation (see text).

can be recognized in the reflectivity spectrum of $Bi_{12}GeO_{20}$,[9] except for the low-energy peak A, which is not resolved, indicating a general, common origin for the electronic transitions.

As a first approximation, BGO can be envisaged as an ionic compound $Bi^{3+}{}_4(GeO_4)^{4-}{}_3$. The crystal structure is isomorphic to eulytine ($Bi_4Si_3O_{12}$) and is characterized by $(GeO_4)^{4-}$ skewed tetrahedra which surround the bismuth ions octahedrally in an irregular manner.[10,11] Relevant distances, calculated by Fisher and Waldner,[11] are presented in Table II. In eulytine the bond lengths Si—O and O—O within each tetrahedron are very close to the values found in other silicates.[12] For germanates such a comparison is not available. In a study of the force constants and chemical bonds of the $(SiO_4)^{4-}$ and $(GeO_4)^{4-}$ anions, Handke[13] used 1.75 Å for the Ge—O bond length. For this reason we think that the electronic properties of $Bi_4Ge_3O_{12}$ can be deduced from the energy levels of the single $(GeO_4)^{4-}$ tetrahedron, modified by the presence of the other tetrahedra and of the Bi^{3+} ions. In a study of the optical phonons in BGO single crystals, Couzi *et al.*[14] used a similar approach, and interpreted the infrared and Raman spectra separating the vibration modes into "internal" vibrations of the GeO_4 groups, comparable to those of different orthogermanate compounds, and "lattice" vibrations, corresponding to the motions of the whole GeO_4 tetrahedra against the Bi^{3+} ion sublattice. Couzi *et al.*[14] caution that such a separation is only ideal, since not always can it be well defined.

TABLE II. Relevant shortest distances (in Å) between atoms in $Bi_4Ge_3O_{12}$, calculated using the crystal parameters reported in Ref. 11.

Ge–O	1.736	
O–O(1)	2.777	Within tetrahedron
O–O(2)	2.777	
O–O(3)	2.946	
O–O	2.794	Nearest tetrahedron
	2.908	
Bi–O(1)	2.149	
Bi–O(2)	2.620	
Bi–Ge	3.584	
	3.681	
Bi–Bi	3.873	

A. Band model

In the $(GeO_4)^{4-}$ ion, the O 2*s* levels lie deeper and are likely to form four localized bands, only slightly hybridized with the Ge 4*s* states. The O 2*p* states split into two main groups of states: the π states are perpendicular to the Ge—O bonds, and form a group of eight nonbonding states; the σ states are directed along the Ge—O bonds and are hybridized with the Ge (sp^3) hybrids, generating a set of four bonding states lying below the O π bands, and four antibonding states lying at higher energies.[15] The latter antibonding states are empty. This qualitative description of the $(GeO_4)^{4-}$ states is supported by the complete neglect of differential overlap (CNDO) calculations of Hojer *et al.*,[16] who obtained three main groups of states, with an average separation from each other approximately of 18 eV. The lowest-energy group is formed by the O 2*s* states; the intermediate group contains the oxygen π and bonding σ states and is about 6 eV wide. The empty antibonding σ states lie at the highest energies.

The energy levels of the germanate ions are further split and spread into bands in the BGO crystalline environment. Probably the largest distortion occurs for some O π states. In fact, inside the single tetrahedron the O—O bonds are not all equal, but one of them is significantly longer than the two others (see Table II), whereas the shortest O—O distance between two tetrahedra is almost the same as that within the single tetrahedron. Thus, we expect that two O π states for each germanate group may split from the other π states, generating a group of bands at higher energy. The bismuth ions contribute with the occupied 6*s* states and the empty 6*p* states. According to Moncorgé *et al.*,[3] who performed a calculation of the energy levels of the $(BiO_6)^{9-}$ cluster, the Bi occupied 6*s* states lie at higher energies than the O 2*p* states, forming the top of the valence bands. The first empty states derive from the Bi 6*p* states and the antibonding combination of the O 2*p* σ states with the Ge ($sp3$) hybrids. The expected level scheme is presented in Fig. 5.

B. The *A* – *H* peaks

We assign the first, sharp peak (peak *A* in Figs. 1 and 2) at 4.78 eV at 80 K in the reflectivity spectrum to an excitonic transition, in agreement with previous suggestions.[2,3,7] Several clues support such an interpretation.

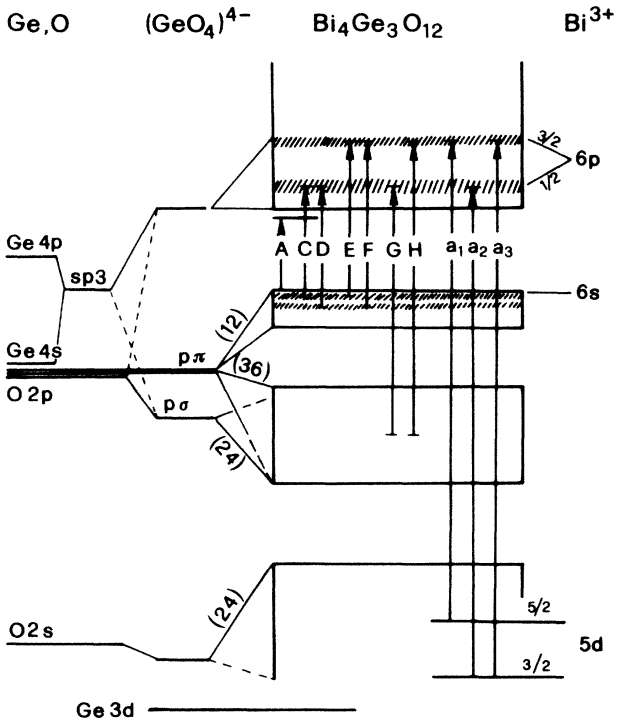

FIG. 5. Energy-band diagram proposed for $Bi_4Ge_3O_{12}$. The Ge and O atomic levels are indicated on the left and their mixing in the $(GeO_4)^{4-}$ tetrahedral complex is indicated schematically in the center (see Ref. 15). The proposed energy-band diagram is drawn on the right together with the assignment of the optical structures (vertical arrows). The hatched areas correspond to peaks of the density of states. The numbers in parentheses give the number of electrons per molecule that fill each group of bands. The separations between the bands and their widths have been derived empirically from the analysis of the optical spectra.

The sharpness of the feature, its shift to higher energies, and its narrowing for decreasing temperatures are typical for excitonic transitions. The shift of the absorption threshold from room temperature (4.22 eV) to 10 K (4.46 eV) found by Rogemond *et al.*[2] is in agreement with the values that can be deduced from the absorption spectra (4.10 and 4.35 eV at RT and 80 K, respectively) that we calculated from the reflectivity spectra. This temperature dependence of the threshold is caused in part by the shift of the first absorption peak from 4.74 to 4.81 eV, and in part to the narrowing of the structure at lower temperatures. In Fig. 6 we compare the spectrum of the absorption coefficient that we derived from the reflectivity data with the excitation spectrum of BGO (Refs. 2 and 6) near threshold. A dip occurs in the excitation spectrum at the same energy as the absorption peak. The same coincidence occurs also in the room-temperature spectra (not shown in Fig. 6). This behavior is similar to that of the first excitonic transition of oxides and of alkali halides.[17] The two-photon excitation spectrum[7] shows only a weak structure at the absorption peak energy, indicating a transition forbidden in two-photon absorption spectroscopy, as for the 1*s* excitons of other compounds.

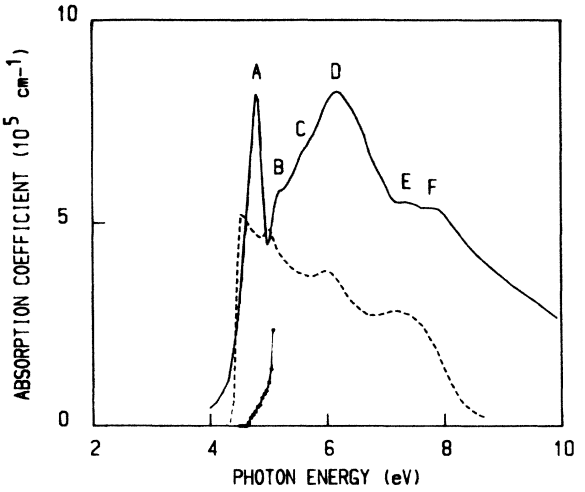

FIG. 6. Spectrum of the absorption coefficient of $Bi_4Ge_3O_{12}$ around the fundamental threshold as derived from the Kramers-Kronig transformations of the 80 K reflectivity spectrum (solid line). For comparison we show also the 10-K one-photon (dashed line, Ref. 2) and the 80-K two-photon (dotted line, Ref. 7) luminescence excitation spectra.

The second group of structures $B-F$ between 5 and 10 eV may be assigned to the interband transitions beginning in the highest O $2p$ π band of Fig. 5 to the conduction bands. The two-photon excitation spectrum measured by Casalboni *et al.*[7] shows a steep increase starting at about 5 eV at 80 K, in correspondence to our dip at 4.96 eV, that we attribute to the fundamental gap of $Bi_4Ge_3O_{12}$. The N_{eff} spectrum shown in Fig. 3 is approaching saturation around 12 eV. We have modeled the shape of the N_{eff} spectrum using the empirical relation

$$N_{\text{eff}}=\begin{cases}0, & E\le E_0\\ N_0\dfrac{\pi}{2}\tan^{-1}\left[\dfrac{E-E_0}{\Gamma}\right], & E>E_0\ ,\end{cases} \tag{1}$$

where E_0 is the absorption threshold energy, Γ a broadening parameter, and N_0 the limit value. In Fig. 4 we show with dashed lines the spectra of N_{eff} calculated with Eq. (1) for the first exciton peak, for the intermediate transitions $B-F$ and for the higher energy transitions G and H. The saturation value that we find from Eq. (1) for the exciton and the intermediate transitions is 18 electrons/molecule, indicating that the oscillator strength for exciting the highest bands derived from the Bi 6*s* states and the O split π bands (see Fig. 5) is almost exhausted.

From Table I we deduce a separation of 0.5 eV for both the C-D and E-F structures, as if they were doublets originating from a splitting of the valence bands density of states. Instead, the B, C-D, and E-F structures may reflect peaks of the conduction-band density of states. The absorption coefficient spectrum as well as the N_{eff} spectrum begin to increase steeply again at about 10 eV. The excitation of deeper valence states, possibly the other O π states and the bonding O σ states, generate the broad

structure G, with maximum around 14.7 eV. As already mentioned, all these states are grouped together within approximately 6 eV in the $(GeO_4)^{4-}$ cluster, and we do not expect to observe fine structures related to details of the valence-band density of states. The broad peak G and the shoulder H might be associated with two peaks of the conduction-band density of states separated approximately by 2 eV. Also the reflectivity spectra of $Bi_{12}GeO_{20}$ (Ref. 9) and of GeO_2 (Ref. 18) present a broad band between 10 and 20 eV, probably due to the excitation of O bonding states. In support to our assignment, we recall that Tojima *et al.*[19] assigned the broad feature present in the reflectivity spectra of $BaPb_{1-x}Bi_xO_3$, with maximum at about 20 eV, to the excitation of the O $2p$ bonding bands. From Eq. (1) we deduce that all these transitions contribute with approximately 80 electrons/molecule, which almost saturates the valence-state oscillator strength (we attribute the small difference to possible errors in the reflectivity spectrum and/or in the Kramers-Kronig transformations), but at 25 eV the oscillator strength is not yet exhausted.

C. The a_1-a_3 bands

A new group of sharp structures appears in the reflectivity spectrum of BGO between 24 and 35 eV, labeled a_1,a_2,a_3 in Fig. 1. In the absorption coefficient spectrum, derived from the Kramers-Kronig transformations of the reflectivity, these features have the typical Fano line shape[20]

$$\mu(E)=\mu_0(E)\left[1+\rho^2\frac{q^2-1+2q\varepsilon}{1+\varepsilon^2}\right] \quad (2)$$

of a discrete transition resonant with a continuum. In Eq. (2) μ_0 is the absorption coefficient of the continuum, $\varepsilon=(E-E_r)/(G/2)$ is a reduced energy with E_r being the resonance energy of the discrete transition and G the linewidth determined by autoionization. q is the profile index determining the distortion of the line and its square is proportional to the relative oscillator strength of the resonant discrete state and the continuum states. ρ^2 is a term representing the fraction of μ_0 which is capable of interference with the discrete state. In Fig. 7 the absorption coefficient spectrum is compared with a curve synthesized using the parameters listed in Table III. In calculating the theoretical curve, we noticed that the values of ρ were very sensitive to the extrapolated continuum background. Thus the values reported in Table III are not fully reliable. Instead, the transition energies and the linewidths depend on the shape of the resonance, and their values are more significant.

We expect two core thresholds between 25 and 35 eV: the Bi $5d_{3/2}5d_{5/2}$ states at (24.4–26.5)±0.5 eV,[21] and the Ge $3d$ states at 28.7±0.7 eV.[21] In the ionic compounds BiI_3 and BiOI, the excitation of the Bi $5d$ electrons produces three sharp features at about 27, 29, and 30 eV, assigned to the Bi $5d_{5/2}$-$6p_{3/2}$, $5d_{3/2}$-$6p_{1/2}$, and $5d_{3/2}$-$6p_{3/2}$ transitions, respectively.[22] Instead, the Ge $3d$ spectrum shows only broad structures, assigned to transitions to a high density of conduction states, with a threshold at about 30 eV.[23] From the comparison with the above

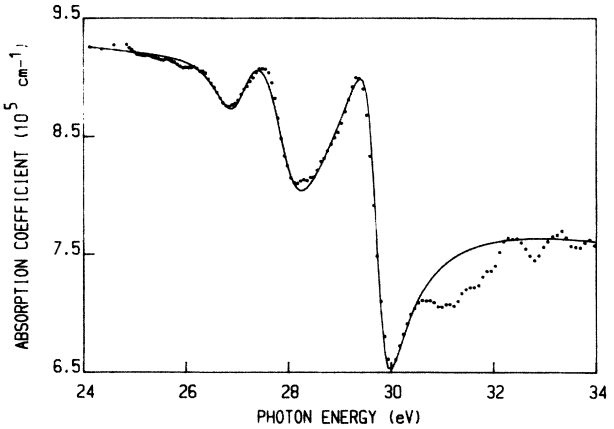

FIG. 7. Absorption spectrum of $Bi_4Ge_3O_{12}$ around the Bi $5d$ threshold obtained from the Kramers-Kronig transformation of the reflectivity spectrum measured at 80 K (dots), compared with a model calculation of the Fano resonances (solid line).

measurements, we suggest that the sharp structures a_1,a_2,a_3 should be assigned to the Bi $5d$ core excitons. The separation between the a_1 and a_3 structures yields a spin-orbit splitting of the Bi $5d$ level of 2.8±0.1 eV, which compares well with the splitting found in other Bi ionic compounds.[22,24] Instead we obtain 1.8±0.1 eV for the spin-orbit splitting of the Bi empty $6p_{1/2}$-$6p_{3/2}$ states, which is larger than the value obtained by Bordas *et al.*[22] in BiI_3. A strong variation of the relative intensities of the Bi $5d$ core excitons was found in different Bi compounds and related to the mixing of the final Bi $6p$ states with the O $3s$ conduction states in BiOI, leading to a delocalization of the Bi $6p$ states.[22] The relative intensities of the a_1,a_2,a_3 structures differ from those of BiI_3 and BiOI, indicating a different amount of delocalization of the Bi $6p$ states in $Bi_4Ge_3O_{12}$. It is worth noticing that the two doublets C-D and E-F, that we have already associated with two peaks of the conduction-band density of states, are separated by 1.8 eV. Also the two broad structures G and H suggest the same conclusion. The coincidence of the value of these separations with the splitting of the Bi $6p_{1/2}$-$6p_{3/2}$ states determined above might not be fortuitous. It could indicate that all these structures are caused by the same two peaks of the conduction-band density of states, corresponding to the delocalized Bi $6p_{1/2}$-$6p_{3/2}$ states, as suggested in Fig. 5.

The Fano line shape that we have synthesized differs significantly from the experimental spectrum between 30 and 32 eV. This difference must be taken cautiously due

TABLE III. Values of the parameters used to synthesize the line shape of the a_1,a_2,a_3 structures with three Fano line shapes, shown in Fig. 7.

	E_r	G	q	ρ	Assignment
a_1	26.94±0.05	0.9	+0.12	0.28	$d_{5/2}$-$p_{3/2}$
a_2	27.90±0.05	1.2	−0.70	0.34	$d_{3/2}$-$p_{1/2}$
a_3	29.72±0.05	0.6	−0.885	0.42	$d_{3/2}$-$p_{3/2}$

to the difficulty in reproducing the background absorption. Nevertheless, we think that it is due to the presence of other structures, possibly transitions from the Ge $3d$ states. Between 25 and 30 eV the N_{eff} spectrum shows again a further increase, due to the new set of transitions.

IV. CONCLUDING REMARKS

We have discussed our model considering the levels of the germanate ions $(GeO_4)^{4-}$ and of bismuth ions Bi^{3+}, but we believe that the optical properties of BGO should be interpreted more correctly by bandlike states, in particular for the conduction-band states. We believe that the description of the three resonances with the Fano line shape, assigned to Bi $5d$-$6p$ transitions, could be more accurate if we introduce a broad and structured density of states of the conduction band.

The good agreement with our simple model of the number of electrons N_{eff} participating in the transitions of the various groups of bands further supports a valence-band scheme of the kind described in Fig. 5. Unfortunately the lack of precise band calculations prevents us from determining the exact nature of the excitonic structure at 4.1 eV.

We believe that our extended reflectivity measurements and the determination of the other optical constants of BGO will be crucial for a better and more complete understanding of the electronic properties of this important material.

*Present address: Dipartimento di Energetica, Universitá degli Studi di Roma I, La Sapienza, via A. Scarpa 14, I-00167 Roma, Italy.

[1]C. L. Melcher, J. S. Schweitzer, A. Liberman, and J. Simonetti, IEEE Trans. Nucl. Sci. **32**, 529 (1985); E. Dieguez, L. Arizmendi, and J. M. Cabrera, J. Phys. C **18**, 4777 (1985); F. Rogemond, C. Pedrini, B. Moine, and G. Boulon, J. Phys. Suppl. **46**, C7-459 (1985).

[2]F. Rogemond, C. Pedrini, B. Moine, and G. Boulon, J. Lumin. **33**, 455 (1985).

[3]R. Moncorgé, B. Jacquier, G. Boulon, F. Gaume-Mahn, and J. Janin, J. Lumin. **12/13**, 467 (1976).

[4]D. P. Bortfeld and H. Meier, J. Appl. Phys. **43**, 5110 (1972).

[5]M. J. Weber and R. R. Monchamp, J. Appl. Phys. **44**, 5495 (1973).

[6]R. Moncorgé, B. Jacquier, and G. Boulon, J. Lumin. **14**, 337 (1976).

[7]M. Casalboni, R. Francini, U. M. Grassano, C. Musilli, and R. Pizzoferrato, J. Lumin. **31/32**, 93 (1984).

[8]F. Antonangeli, M. Piacentini, and N. Zema (unpublished).

[9]Sh. M. Efendiev, A. M. Mamedov, V. E. Bagiev, and G. M. Eivazova, Zh. Tekh. Fiz. **51**, 1755 (1981) [Sov. Phys.—Tech. Phys. **26**, 1017 (1981)].

[10]See, for example, M. A. Durif, C. R. Hebd. Seances, Paris **244**, 2815 (1957); R. Nitsche, J. Appl. Phys. **36**, 2358 (1965).

[11]P. Fisher and F. Waldner, Solid State Commun. **44**, 657 (1982).

[12]J. V. Smith and S. W. Bailey, Acta Crystallogr. **16**, 801 (1963).

[13]M. Handke, J. Mol. Struct. **114**, 187 (1984).

[14]M. Couzi, J. R. Vignalou, and G. Boulon, Solid State Commun. **20**, 461 (1976).

[15]See, for example, W. A. Harrison, *Electronic Structure and the Properties of Solids* (Freeman, San Francisco, 1980), p. 258.

[16]G. Hojer, S. Meza-Hojer, and G. Hernandez de Pedrero, Chem. Phys. Lett. **37**, 301 (1976).

[17]N. Itoh, Adv. Phys. **31**, 491 (1982).

[18]L. Pajasová, Czech. J. Phys. B **19**, 1265 (1969).

[19]S. Tajima, H. Ishii, A. Masaki, S. Uchida, K. Kitazawa, S. Tanaka, M. Seki, and S. Suga, Activity Report of Synchroton Radiation Laboratory, Institute for Solid State Physics, University of Tokyo, 1986 (unpublished).

[20]U. Fano, Phys. Rev. **124**, 1866 (1961).

[21]J. A. Bearden and A. F. Burr, Rev. Mod. Phys. **39**, 125 (1967).

[22]J. Bordas, J. Robertson, and A. Jakobsson, J. Phys. C **11**, 2607 (1978).

[23]M. Taniguchi, S. Suga, S. Shin, K. Inoue, M. Seki, and H. Kanzaki, Solid State Commun. **44**, 85 (1982).

[24]S. P. Kowalczyk, L. Ley, F. R. McFeely, and D. A. Shirley, Solid State Commun. **17**, 463 (1975).